VLF emissions from the magnetosphere

A computer simulation shows how very-low-frequency emissions can be triggered in the magnetosphere and then propagate as "whistlers."

Ravindra Nath Sudan and Jacques Denavit

From the earliest days of radio experimentation, various kinds of very-lowfrequency electromagnetic radiation have intrigued those who heard the strange mixture of glissandi whistles, hisses, chirps and warbling sounds on their headphones. One common type sounds like birds awakening in the morning and was appropriately named the "dawn chorus." Confined usually to an audiofrequency range of 200 to 30 000 Hz, these emissions appeared to be distinct from other forms of "static" -locally initiated noise due to nearby lightning strokes, precipitation, or man-made electrical interference. The observational equipment required for the study of such emissions is comparatively simple-a single-turn loop antenna connected to a high-gain, lownoise, wide-band audio amplifier. If the output is recorded on magnetic tape, spectrograms can be produced by standard techniques. Time markers can be added either from a local clock or from a radio station.

We now know that these emissions propagate through the earth's magnetosphere, and we can distinguish two main types. One kind, the "whistlers," consists of bursts of radiation beginning at high frequency and gliding down to about 1000 Hz in a period of about one second; they originate with lightning strokes in the atmosphere and propagate between magnetically conjugate points in the northern and southern terrestrial hemispheres. The other kind-broad-band low-frequency hiss and the narrow-band discrete emissions of which the dawn chorus is an example-apparently originates in the magnetosphere. Discrete emissions need to be triggered by some other phenomena, and the triggering mechanisms for this type of VLF magnetospheric emission include whistlers and powerful audiofrequency transmitters. In this article we will be considering a theory that accounts for such artificially triggered emissions and the results of some numerical simulations that test the validity of the theory.

Whistlers

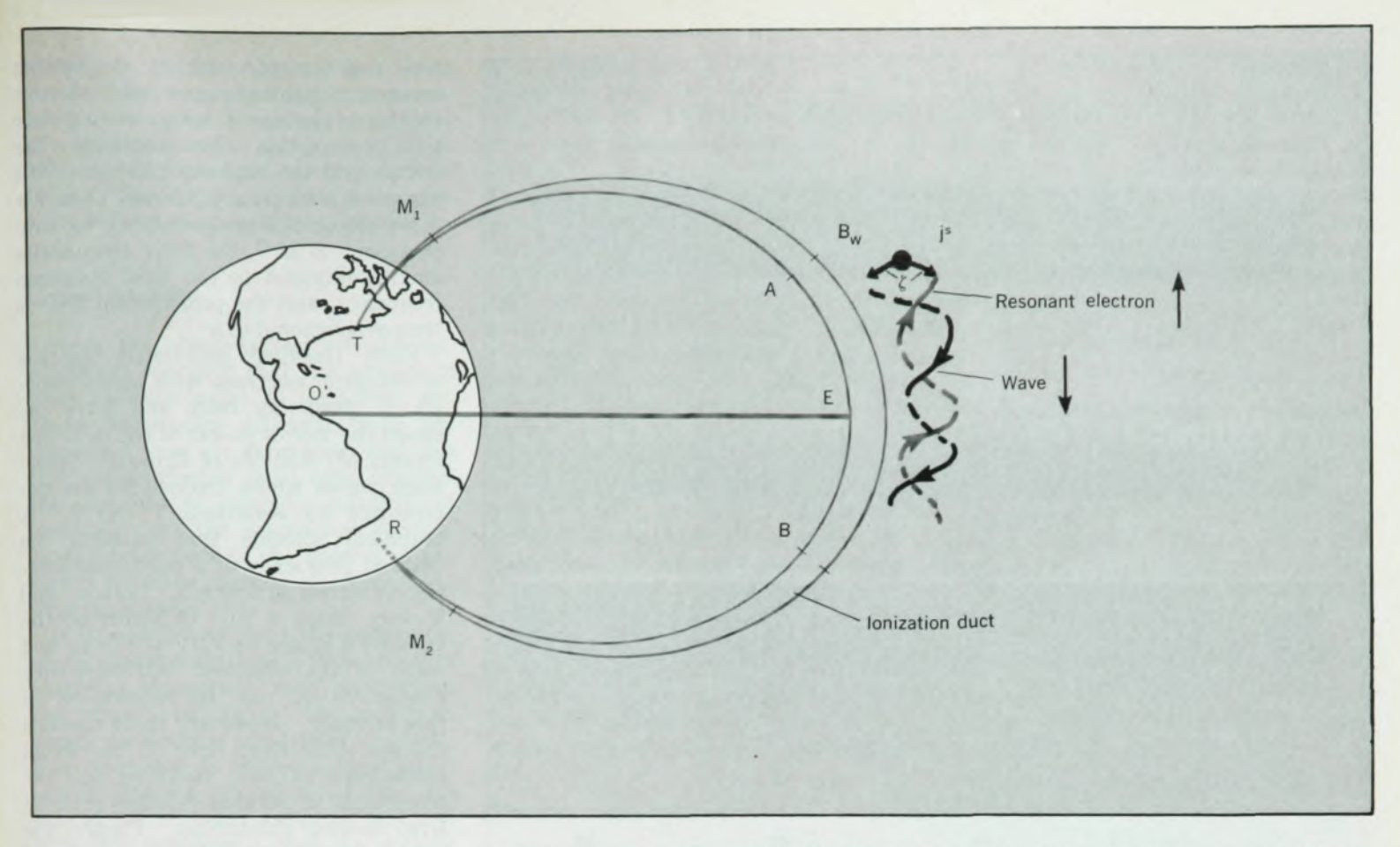
Whistlers are now relatively well understood, and the history of observations goes back as far as 1894 to the period of pioneers in radio-wave propagation.¹ The detailed study of whistlers in recent times begins with L. R. O. Storey's classic work² of 1953. Under suitable conditions a fraction of the electromagnetic energy radiated from a lightning stroke is refracted into

the ionosphere along the geomagnetic field. This energy propagates as a right-circularly polarized electromagnetic wave with phase and group velocities much below the light velocity c. This "whistler" mode is familiar to solid-state physicists as a "helicon." The wave energy is guided in a duct along the lines of force of the geomagnetic field by field-aligned enhancement of ionization³ that acts as a "whispering gallery" for these waves (see figure 1). Ground-based stations receive the wave energy mostly through such ducts, whereas satellite observations are not so limited. Wave energy suffers a dispersion because of the magnetized free electrons of the magnetospheric plasma, which cause the high-frequency components to travel much faster than the low-frequency components and results in the characteristic descending tone of a whistler.

Sometimes trains of whistlers are observed following each other at equal time lapses but with the rate of frequency decrease less in each successive echo. The explanation is that a fraction of the wave energy is reflected at the ends of the propagation duct, where the wave enters the lower ionosphere. The dispersion increases for the subsequent echoes because of the longer propagation path.

Many whistlers are preceded by a sharp click that signifies the particular

Ravindra Nath Sudan is professor of applied physics and of electrical engineering at Cornell University, Ithaca, N.Y., and Jacques Denavit is professor of mechanical engineering and astronautical sciences at Northwestern University, Evanston, III.



A field-aligned ionization duct, TER, along which a particular whistler generated at T propagates. The region where it could trigger VLF emissions is AB; M_1 , M_2 are the mirror points of an electron resonant with the whistler. Note that the resonant electron moves opposite in direction to the whistler.

lightning stroke that generates the whistler; for nearby strokes the frequency components of the click travel to the observer by a direct path in the earth-ionosphere waveguide, and hence suffer little or no dispersion. When no click is observed the whistler has its source in the opposite hemisphere at the magnetic conjugate point. On occasion the wave energy travels in several neighboring ducts, each with slightly This different propagation times. gives the appearance of several overlapping whistlers, known as "multiple whistlers.

Very-low-frequency emissions that originate in the magnetosphere are less well understood. The bewildering variety of characteristics that these emissions show has been documented in detail by Robert Helliwell.1 They can be divided into two main classes: lowfrequency (less than a few kHz) broadband emission known as "hiss," and narrow-band discrete emissions. Quite often VLF emissions are associated with whistler echo-trains,4 and indeed appear to be triggered by them. This type occurs more frequently during periods of high magnetic activity and is restricted to higher geomagnetic latitudes.

Figure 2a shows an example of "hiss" with the upper cut-off frequency at 3 kHz. A careful examination of frequency-time recordings reveals that

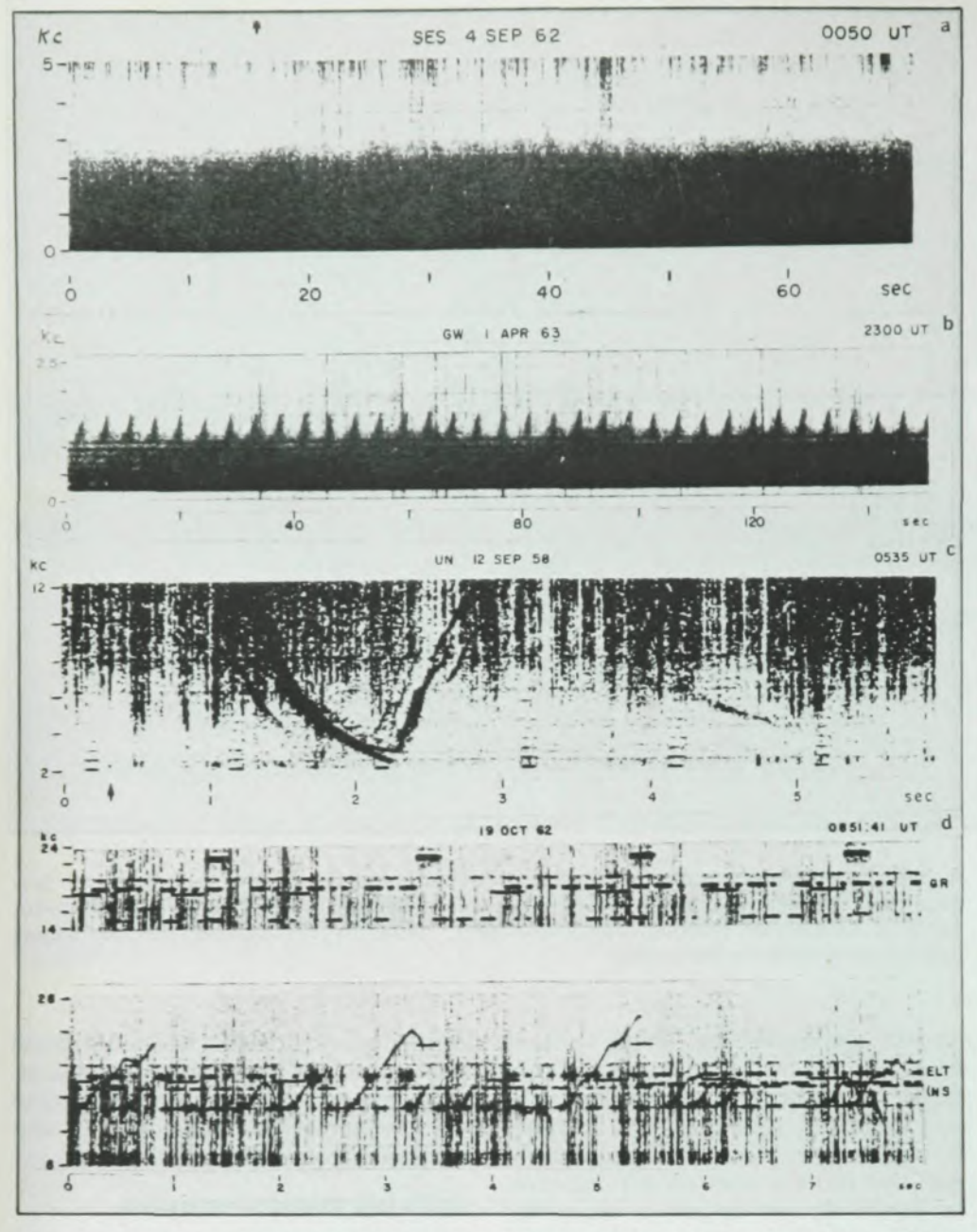
discrete emissions are almost always triggered by another disturbance. In figure 2b we have an example of periodic emissions in which each emission is triggered by the previous emission, and the process goes on for minutes. In figure 2c we notice a rising-frequency emission triggered by a lightning-generated whistler towards its low-frequency trailing end.

Whistler waves can also be generated artificially by powerful audiofrequency transmitters. An important clue in the understanding of the origin of VLF emissions was provided by the observations of Helliwell and his coworkers5 that such ground-based radio-transmitter signals could trigger emissions if some of the signal energy travels in the whistler mode along a field-aligned ionization duct in the magnetosphere (figure 1). Figure 2d shows such emissions triggered by morse-code signals from Station NAA at 14.7 kHz and observed on board the ship Eltanin in the South Polar region. Because these emissions are stimulated by a signal whose main characteristics are known a theoretical treatment is made possible. We will confine ourselves here to a description of our current understanding of the mechanism of this particular triggering process. A theory that can reasonably account for this feature can then be extended to cover the variety of other naturally occurring emissions. It should be remembered that once generated these emissions propagate exactly as whistlers do, and the energy reaches the ground only if it is trapped in the ionization ducts.

Artificially triggered emissions

The salient features of these emissions can be noticed in the frequencytime recordings of figure 2d and are summarized as follows:

- A minimum pulse length is required for triggering emissions. Thus, emissions were recorded from a 10⁶-watt transmitter radiating at 14.7 kHz for 150-millisec pulse length, but 50-millisec pulses were almost never successful in triggering emissions. In the case where emissions are caused by a train of naturally occurring whistlers, the emissions are triggered towards the low-frequency tail, where the rate of change of frequency becomes small as result of dispersion.
- The energy released in triggered emissions may exceed that in the triggering pulse, which indicates that an external source of energy is required—for example, the 5-10-keV energetic electrons in the magnetosphere.
- ▶ Emissions originate at the frequency of the triggering signal, or perhaps a few hundred hertz above it. In most cases their frequency increases by about 10–50% in times of the order of a



Ground-based frequency-time recordings of different types of VLF emissions. ("UT" denotes universal time.) Part a "Hiss" with upper cut-off frequency at 3 kHz. (Seattle, Wash.) Part b Nondispersive "periodic emission" with a period of 4.33 sec at 1.5 kHz. (Great Whale River, Quebec) Part c Whistler-triggered emissions; note that the rising emission is triggered toward the low-frequency end of the whistler at 3.2 kHz. The arrow marks the whistler source in time. (Unalaska, Alaska) Part d Artificially triggered emissions from station NAA on 14.7 kHz as observed on the ship Eltanin. Each principal emission is connected with a dash (150 millisec); the dots (50 millisec) are not connected with any emission. Upper spectrogram shows transmitted signals at 14.7 kHz, three dashes followed by three dots. (From R. A. Helliwell, ref. 1.)

fraction of a second; on occasion an initial drop in frequency is followed by a monotonic increase. The frequency-time characteristics may have other more complicated shapes, and the emissions can cease abruptly. Their bandwidth is very narrow, \$\infty\$ 100 Hz.

It was soon recognized that the emissions must result from the interaction of energetic electrons with whistler waves. The kinematics of this interaction are described by the whistler dispersion relation that relates the frequency $\omega/2\pi$ to propagation vector ${\bf k}$

$$\frac{k^2c^2}{\omega^2} = 1 + \frac{\omega^2_{\rm p}}{\omega(\Omega \cos \theta - \omega)}$$
 (1)

and the condition for electron-wave

resonance

$$\omega - k v_{\parallel} \cos \theta = n\Omega \tag{2}$$

Here $\omega_p/2\pi$ and $\Omega/2\pi$ are the plasma and the electron cyclotron frequencies of the ambient plasma, θ is the angle made by the wave normal to the geomagnetic field and \parallel , \perp denote components parallel and perpendicular, respectively, to the geomagnetic field. When n=0 we have the so-called "Landau resonance," and for n=1 we have the cyclotron resonance; that is, for electrons with velocity v given by equation 2 the wave frequency is Doppler-shifted to their own cyclotron frequency.

The whistler mode is strongly disper-

sive, and the characteristic descending tones of a lightning-generated whistler train are accounted for by noting that the propagation time between the source and the receiver increases with decreasing frequency. From equation 1 we obtain the group velocity v_g , proportional to $\omega^{1/2}$, for wave frequencies small compared to the local cyclotron frequency, and the propagation time is thus proportional to $\omega^{-1/2}$.

Early theories⁶ postulated bunches of energetic electrons with mean velocity v bouncing back and forth between the mirror points of the field line (points M₁ and M₂ of figure 1), generating waves whose frequencies are determined by equations 1 and 2. A graphical solution that predicts the emitted frequency at a particular location is shown in figure 3. Both v and Ω vary along a line of force, so the emitted frequencies vary with time and some of the observed frequency-time characteristics can be reproduced in this manner. However, these theories did not shed much light on the actual mechanism of wave emission, and the hypothesis of electron bunches suffered from several difficulties. Firstly, the narrow bandwidth of the emissions demands an inadmissably small spread in v; the ratio $\Delta v / v$ is approximately 10-2. The well known electrostatic two-stream instability7 is expected to spread the beam velocity in time of a few hundred plasma periods $(2\pi/\omega_p)$, so that even if such bunches were to exist they would have a very short lifetime. Furthermore, in a study of periodic emissions (see figure 2b), Neil Brice8 noted that the interval between emissions was not the electron bounce time between mirror points as expected from this hypothesis, but was instead the whistler propagation time.

To circumvent these difficulties Helliwell9 proposed a phenomenological theory in which electron bunches were not assumed to exist ab initio but were supposed to be created by the triggering wave. This theory revived an idea due to Brice8 in which such "bunching" is interpreted as an alignment of the phase of the electron transverse velocity to produce a transverse current that radiates an emission like a radio antenna. Thus a new element was introduced into the kinematics of the problem. In the meantime one of us (Sudan) and Edward Ott10 came independently to the same conclusion. We attempted, however, to clarify the dynamics of wave emission by proposing an instability of the phase-correlated bunch of electrons and obtained quantitative estimates of the rate at which a new emission is generated.

In what follows we give a brief outline of the Sudan-Ott theory¹⁰ and its relationship to Helliwell's⁹ approach. Some of the basic premises and as-

sumptions of the theory have been checked by numerical simulations involving the computation of the motions of a large number of electrons (of order 10⁵) in self-consistent electromagnetic fields. The results of these computations will be discussed later in this article.

Linear instability

From the observations one can immediately conclude that the process of wave emission must be nonlinear, because frequencies different from the triggering wave are generated, and also that such emission must arise through the presence of energetic nonthermal electrons since the second law of thermodynamics forbids the growth of coherent waves in thermal equilibrium to large amplitudes.

It is well known that the magnetospheric plasma contains a population of energetic electrons11 with energies in the range 1-103 keV. The minimum energy an electron must have for cyclotron resonance is obtained from equation 2, and for typical conditions this falls in the 1-10-keV range so that it is with this component that we will be principally concerned. In the region where the emissions may be presumed to originate (see figure 1) the energy density of the geomagnetic field $B_0^2/8\pi$ is of order 10-6 ergs/cm3, the energy flux density of the energetic electrons is of order 1.0 ergs/cm2/sec, and the observed wave energy flux density is of order 10-6 ergs/cm²/sec. It must be kept in mind in what follows that the energetic electrons have an energy density far in excess of that in the waves.

These electrons are trapped in the geomagnetic field by virtue of the fact that both the kinetic energy E and $\mu = (1/2) m v_{\perp}^2 / |\mathbf{B}|$, the magnetic moment, can be considered constants of motion. There is, however, a group of electrons with E and μ such that they pass through the mirror points of the magnetic field and are lost. Thus the trapped distribution is not isotropic, and the mean perpendicular energy Ei for this distribution can exceed the mean parallel energy E; in other words, the population is inverted and may be spontaneously unstable as it is in lasers. A number of investigators working independently (Roald Sagdeev and V. D. Shafranov, 12 Sudan, 13 Peter Noerdlinger,14 and Timothy Bell and Oscar Buneman¹⁵) showed that such a distribution is in fact unstable, and indeed such a medium acts as an amplifier for whistler waves. The conservation of energy and parallel momentum for a resonant electron requires

$$\hbar\omega + \Delta E_{\perp} + \Delta E_{\parallel} = 0 \tag{3a}$$

$$\hbar k_{\parallel} + m\Delta v_{\parallel} = 0 \tag{3b}$$

and, recalling that $\omega = k_{\parallel}v_{\parallel} + \Omega$ for resonance, we obtain $\Delta E_{\perp} = -\hbar\Omega$ and $\Delta E = \hbar k |V|$. Thus a resonant electron loses perpendicular energy $\hbar\Omega$ to release a quantum of whistler energy $\hbar\omega$, and the excess goes to increase the parallel energy. This interaction reduces the pitch angle α of the electron (tan $\alpha = v_{\perp}/v$) and it is conceivable that the resonant electron could lose confinement. When such resonant electrons lose confinement they are precipitated into the upper atmosphere. Balloon-mounted observations in the south polar regions have shown a strong correlation between emissions and bursts of x rays emitted by these electrons.16 precipitated resonant Charles Kennel and Harry Petschek17 have proposed this self-limiting mechanism to establish the upper bound of trapped energetic electron flux. A detailed calculation¹³ shows frequencies up to $\Omega(1 - E_{\perp}/E_{\perp})$ are unstable, which may explain some of the observed broad-band hiss, with a sharp upper frequency cut-off (figure

Electron trapping in waves

This linear instability by itself cannot provide the basis for the understanding of triggered discrete emissions, because it accounts for the amplification of the triggering signal but not the creation of additional frequencies. One is therefore forced to consider nonlinear processes, and, in particular, those that limit the amplitude of the growing wave. Since the instability is derived from a linearized analysis, departures from its predictions will

occur if the fundamental assumption of linearization are violated. This will be the case when the orbits of the resonant electrons begin to be profoundly affected by the wave electromagnetic field. We can pursue this point by considering the motion of an electron in a finite amplitude right-circularly polarized wave defined through its vector potential

$$\mathbf{A} = A[\hat{\epsilon}_x \cos(k_0 z - \omega_0 t), \\ -\hat{\epsilon}_y \sin(k_0 z - \omega_0 t)]$$

The ratio of the electric to the magnetic field is given by ω_0/k_0c , which is much smaller than unity because of the high dielectric constant of the medium (equation 1) in the frequency range of interest. We may therefore neglect the electric field and consider only the Lorentz force if $\omega_0 \ll k_0v$ where v is the particle speed. Thus

$$\ddot{z} = (ekAv_{\perp}/mc) \sin(k_0 z - \omega_0 t + \phi)$$
 (4)

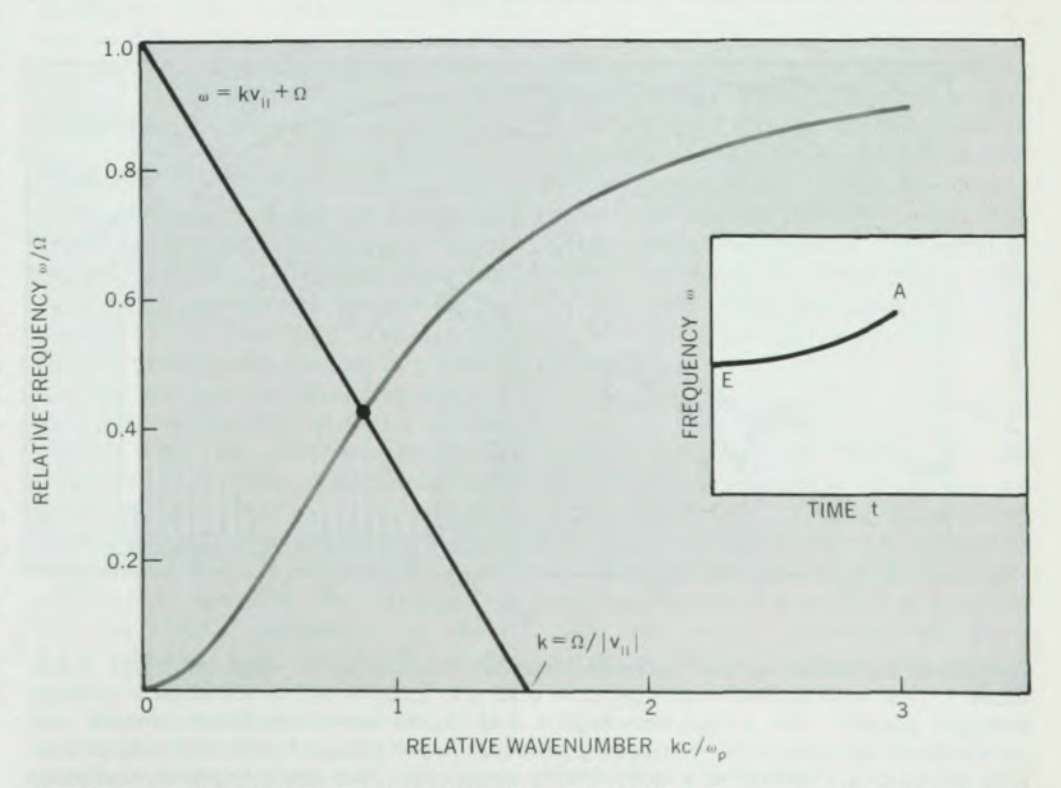
where $v_x = v_\perp \cos \phi$ and $v_y = v_\perp \sin \phi$. The phase of an electron with respect to the wave magnetic field, that is, the angle made by its instantaneous perpendicular component of the velocity \mathbf{v}_\perp to the local direction of the wave magnetic field $B_\mathbf{w} = k_0 A$, is defined by $\zeta = k_0 z + \phi$ (see figure 1). To a resonant particle with

$$\dot{z} \approx (\omega_0 - \Omega)/k_0$$

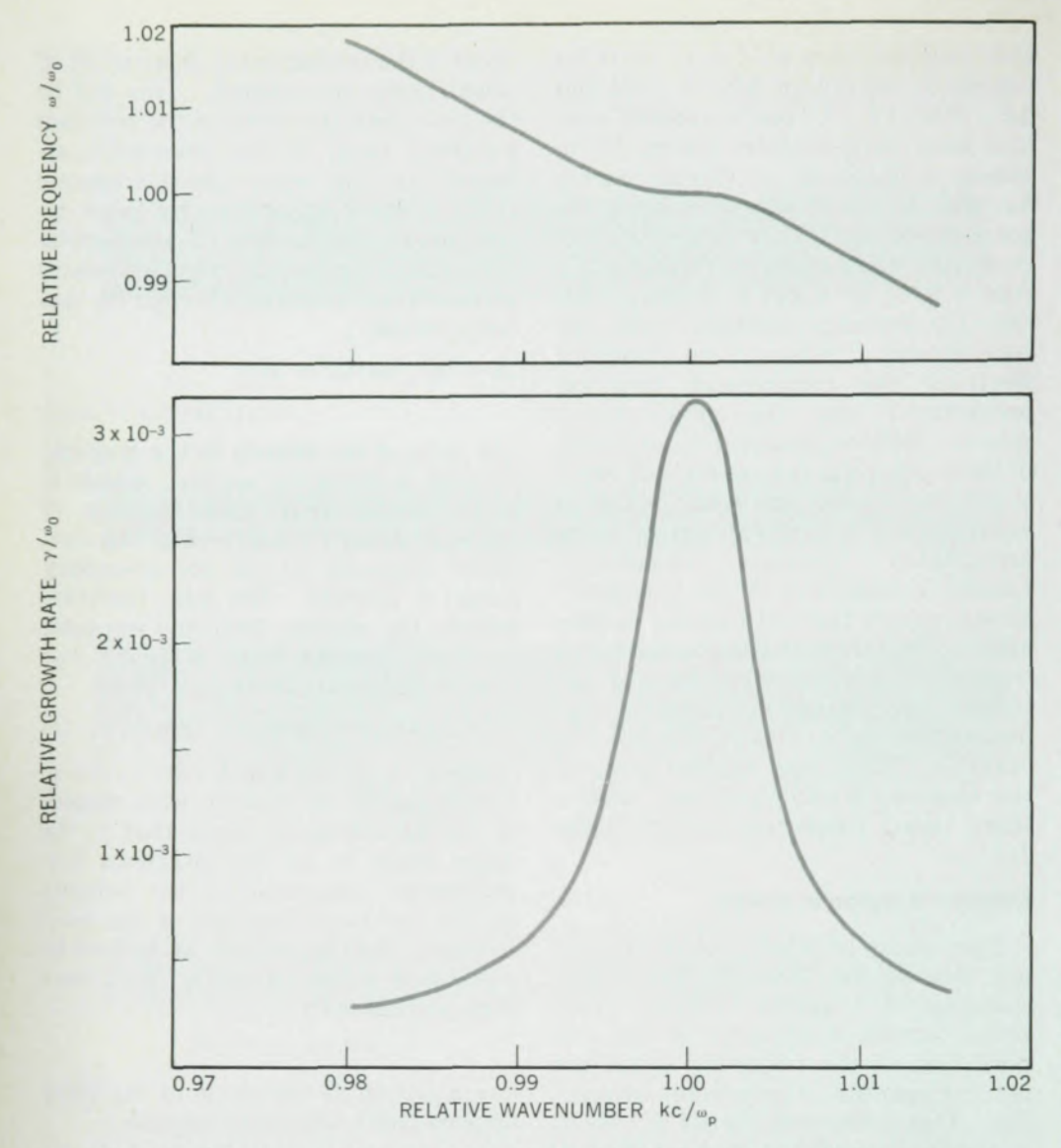
(see equation 2) the phase of the wave appears quasi-stationary because

$$k_0 z - \omega_0 t + \phi \approx 0$$

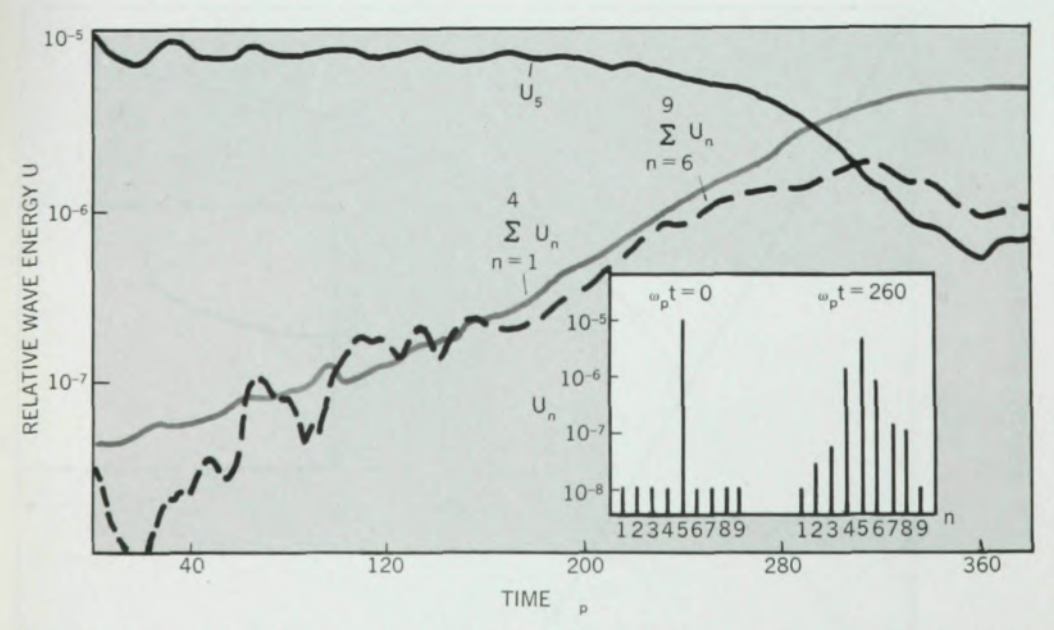
with $\phi \approx \Omega t$. In other words the spiral trajectory of the resonant electron is just in phase with the spiralling-wave



Graphical solution of equations 1 and 2 with n=1 and $\theta=0$. The emitted frequency is determined by the intersection of the two curves. The inset gives a frequency-time curve for an electron bunch travelling from E to A in figure 1.



Growth rate and frequency of waves driven unstable by phase-correlated electrons; parameters are for region AB of figure 1, for the case of figure 2d. OE = 3 × Earth radius, $\omega_{\rm p}/2\pi=180~{\rm kHz},~\Omega/2\pi=35~{\rm kHz},~\omega_0/\Omega=\frac{1}{2},~\omega_{\rm T}/2\pi=50~{\rm Hz},~\langle v_\perp|^2\rangle^{1/2}/c=0.15,~n_{\rm R}/n_0=10^{-7}.$ The maximum value of γ scales as $(n_{\rm R}/n_0)^{1/3}$. Note that the group velocity vanishes where the growth rate is maximum, signifying that this instability is nonconvective, and the unstable region behaves like an oscillator.



Numerical simulation of the correlated-particles instability. A large-amplitude wave, mode n=5, with $B_{\rm w}/B_0=0.1$, $\omega_0/\Omega=0.25$ and $\Omega/\omega_{\rm p}=0.5$ is initialized in a stable energetic plasma. For a short time ($\omega_{\rm p}t=0$ to 15) the wave is cyclotron damped; then its amplitude oscillates with the trapping period $2\pi/\omega_{\rm T}=30~\omega_{\rm p}^{-1}$, and after several trapping oscillations it settles to a quasi-steady amplitude. This wave, however, correlates the phases of resonant electron perpendicular velocities as shown in figure 1, thus forming an unstable distribution. This instability pumps the lower and upper sideband modes from their initial noise levels up to the order of the main-wave amplitude.

magnetic field (see figure 1). Note that for whistlers ω_0 is always less than Ω , and therefore the resonant electron has a negative \dot{z} . This condition means that it always moves opposite to the phase and group velocities of the wavepacket. The resonant electron obeys the oscillator equation 19

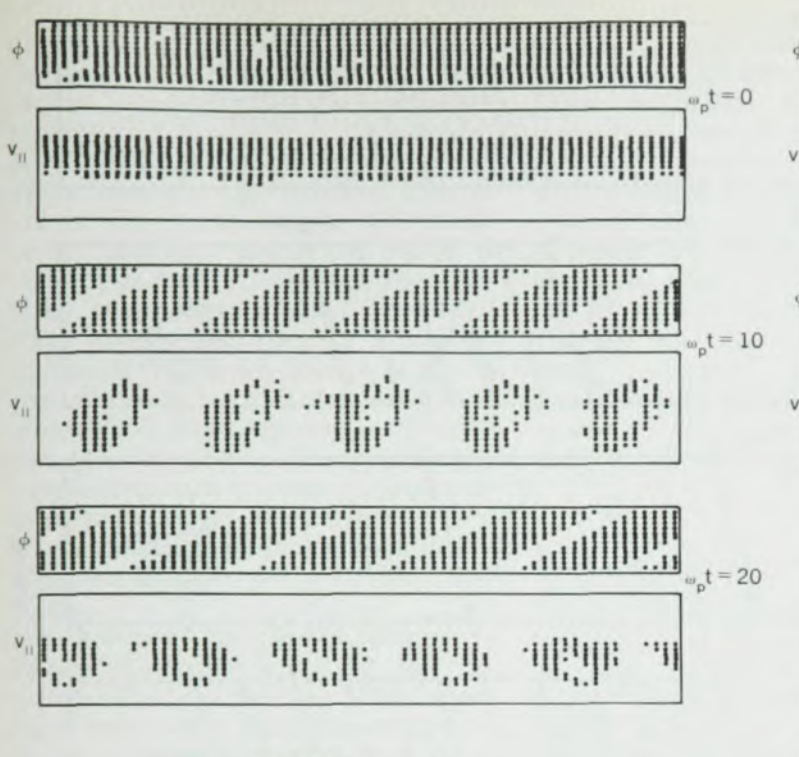
$$\dot{\zeta} = (ek_0^2 A v_\perp / mc) \sin \zeta \equiv \omega_T^2 \sin \zeta \quad (5)$$

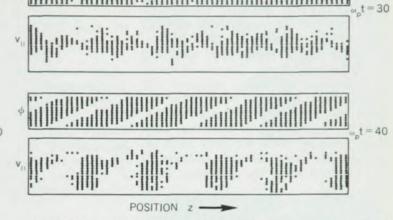
The $v \times B_w$ Lorentz force accelerates the electron in the z-direction, and it comes to an equilibrium with the wave when this force vanishes. For $k_0 > 0$ this occurs when v_{\(\perp}\) is antiparallel to} B_w , that is, when $\zeta = \pi$, and it oscillates about this position at a frequency $\omega_{\rm T}$; the $\zeta = 0$ position is unstable. As a wave packet propagates the incoming resonant electrons have their transverse velocities aligned approximately antiparallel to the wave magnetic field. Such electrons are often described as "trapped"—in analogy to a particle at the bottom of a potential well. As we have noted earlier the resonant electrons move opposite to the wave packet, so that they spend on the average a time

$$T \approx L/(|v|_R + |v|_g)$$

within the wave packet of length L. If the transit time T exceeds $2\pi/\omega_T$ we can expect them to be phase-correlated such that a circularly polarized transverse current is generated (figure 1). This transverse current can be the source of new emissions. The phase correlation can only take place where the gradients in electron density and geomagnetic field are relatively gentle, because otherwise the wave suffers an acceleration or deceleration that results in "spillage" of these resonant electrons from the magnetic "potential whose magnitude is Av_{\perp}/c . Thus these correlated electrons are produced at the magnetic equator near the top of a particular duct along which the triggering wave is propagat-The source of new emissions is in fact located within a fraction of an earth radius on either side of the magnetic equator (figure 1).

We assume that the phase-correlation of this source current is maintained, even as the electrons gradually pass out of resonance with the triggering wave-either because they leave the wave packet or because their parallel velocity changes in the spatially varying magnetic field. This assumption is supported by the results of a computer simulation of a finite-length wavepacket propagating in an unstable medium, to be discussed later. Notice that the phase-correlated electrons may give rise to only a transverse current and not to a space-charge, so that they will not be rapidly dispersed by the electrostatic two-stream instability. This source current js can, of





Resonant electron densities. These plots show particle correlation from the large-amplitude wave shown in figure 5. Position z is plotted horizontally, and regions of higher electron density are shown by dots. The electron density is initially uniform, with only small perturbations due to the main wave current. At $\omega_p t = 10$ and 20 strong phase correlation due to electron trapping is evident on the plots of ϕ versus z, whereas trapping "vortices" are observed on the plots of v versus z. At $\omega_p t = 30$ phase correlation is not apparent because it corresponds to a complete trapping period.

course, create new waves by polarizing the medium. This follows from Maxwell's equation

POSITION z

$$\epsilon \partial \mathbf{E} / \partial t = -4\pi \hat{\mathbf{j}} + c\nabla \times \mathbf{B}_w$$

where $\epsilon(\omega) = 1 + \omega_n^2 / \omega(\Omega - \omega)$

This is the "antenna" effect mentioned earlier.

The rate at which the wave magnetic field $\mathbf{B}_{\mathbf{w}}$ builds up is easily computed to be

$$\frac{d(B_{\rm w}/B_0)}{d(\omega t)} = \frac{n_{\rm R}}{n_0} \frac{\langle {\rm v_\perp}^2 \rangle^{1/2}}{c} \left(1 - \frac{\omega}{\Omega}\right)^2 \left(\frac{kc}{\omega}\right)$$
(6)

where the essential point to note is the linear dependence on n_R/n_0 , the ratio of the density of phase-correlated electrons contributing to js to the total electron density. Now from the meager data20 available on the fluxes of energetic electrons between 1 and 10 keV one estimates a value for $n_{\rm R}/n_0$ that ranges from 10-7 to 10-10. For the emission to reach an amplitude comparable to that of the triggering wave (Bw not greater than 10-7 gauss) one obtains a time of order 3×10^{-3} to 3×10^{-1} sec for this range of $n_{\rm R}/n_0$. Calculations^{9.21.22} based on just this effect are put to some strain to account for the growth time of a few milliseconds demanded by the data (see figure 2d), if the higher values of n_R/n_0 prove to be inadmissable.

問

他们

\$

88

titel

10

A more serious difficulty with these calculations results from the fact that the emitted frequency is determined by the frequency of j^s as observed in the laboratory frame; this frequency is always ω_0 even when the resonant electrons leave the triggering wavepacket. Thus it is not possible to account for the continuously changing frequencies of the emission. Alternatively, the

emitted frequencies do not occur in the frequency bandwidth of the triggering wave. The only source of new frequencies is in the noise spectrum. Thus any theory that purports to explain VLF emissions must contain a physical mechanism that amplifies selectively the thermal noise to observed amplitudes. Such a mechanism is discussed in the next section.

(A detailed calculation²³ in which the trapped electrons have been smeared out in ζ -space shows that unstable sidebands with frequencies $\omega_0 \pm \Delta \omega$, with $\Delta \omega \approx \omega_T/(1 + \Omega/2\omega_0)$, are generated with a maximum growth rate of $1.3\gamma_L$, where γ_L is the linear efolding rate. For the relevant parameters $\gamma_L \approx 10~\text{sec}^{-1}$, which is too slow to explain the observed emissions.)

Phase-correlated instability

It is however possible for the phasecorrelated electrons to emit new waves by the process of coherent emission10 at a faster growth rate proportional to $(n_{\rm R}/n_0)^q$ with q ranging from $\frac{1}{3}$ to $\frac{1}{2}$. In this process the change of phase in the electron motion caused by the very act of wave emission is taken into account. Thus the electrons are phased together and emit collectively with great enhancement in the emission rates. This is in fact the sort of thing that underlies radiation from collective motion of particles, for example in Thomas Gold's explanation of radiowave emission from pulsars.24 A detailed calculation, along these lines, of the interaction of the phase-correlated electrons with the plasma gives a dispersion relation for the emitted waves whose growth rates and frequencies for typical triggered VLF emissions are shown in figure 4. Note that the growth rates are sharply peaked, explaining the narrow frequency spectrum of VLF emissions and that their magnitude is sufficiently large to amplify background noise to adequate levels within a few milliseconds.

In the case of a non-uniform magnetic field the triggering wave propagates with a constant frequency ω_0 , while its wavenumber k_0 becomes a function of the local cyclotron frequency. Resonant electrons participating in the instability at a location z were correlated at an upstream location z_0 and have a velocity

$$v_{\rm R} = \left[\omega_0 - \Omega(z_0)\right]/k_0$$

As stated earlier we assume that the phase correlation of resonant electrons is maintained even as the electrons are gradually passing out of resonance with the triggering wave. This assumption is verified by the computer simulation results to be discussed in the next section. Substitution of the above value of $v_{\rm R}$ into the resonance condition (equation 2) and the assumption $k \approx k_0$ yields

$$\Delta \omega = \omega - \omega_0 \simeq \Omega(z) - \Omega(z_0)$$

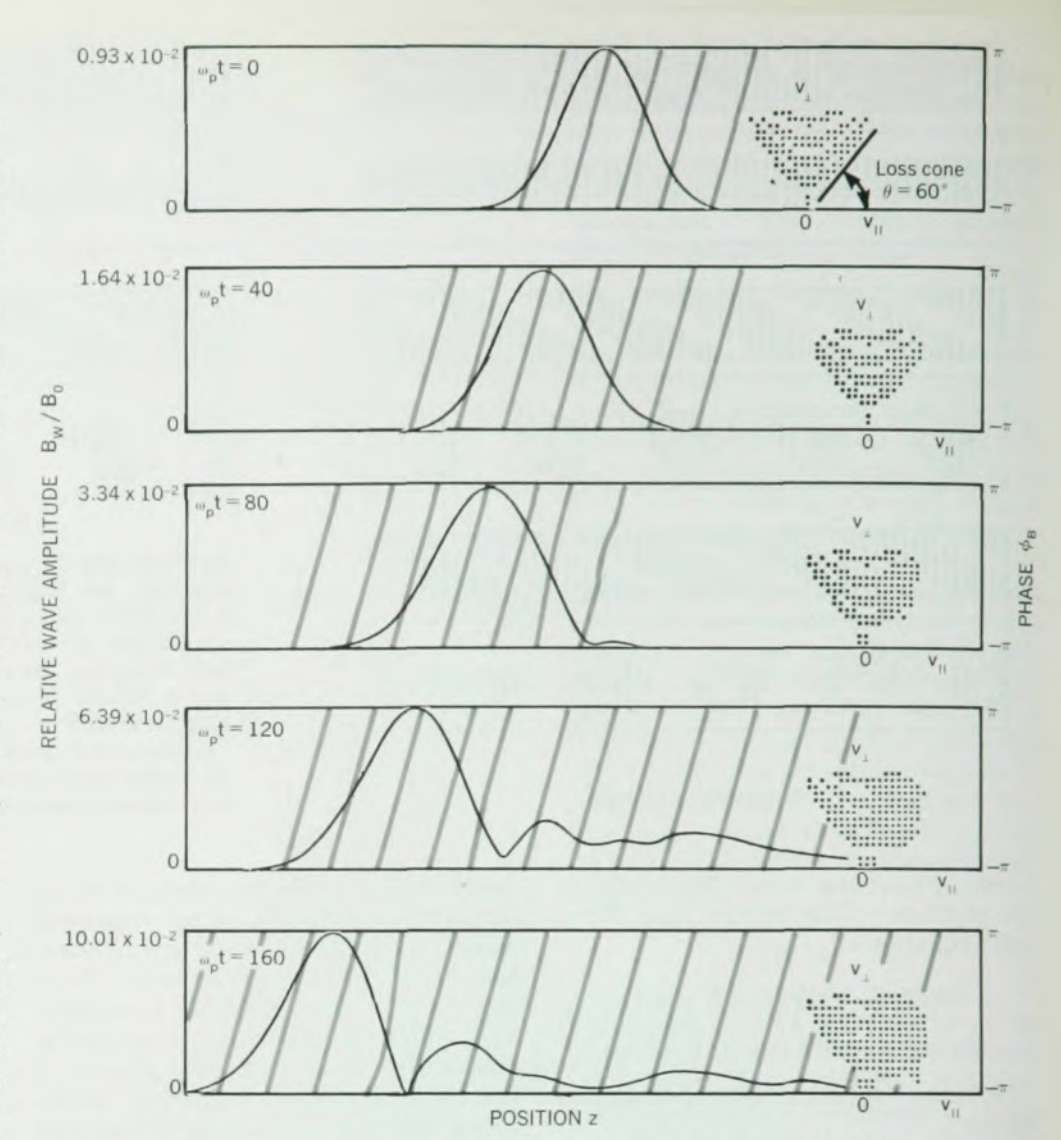
If we assume a transit time of 100 millisec with a resonant velocity $v_{\rm R}$ approximately 3×10^9 cm/sec, the transit distance is 3000 km. At a distance of three earth radii in the equatorial region, the relative change in magnetic field over such a distance can be as large as 15% and therefore accounts for the observed frequency changes in the emitted waves.

Computer simulations

Computer models simulating the dynamic behavior of plasmas may be devised by either numerically solving the collisionless kinetic and Maxwell equations, or by computing the motions of a large number of particles interacting with their self and externally applied electromagnetic fields.²⁵ The results presented in this paper were obtained by the latter method. (Details of these computations are being prepared for publication.) At every time step the fields are computed in terms of the particle velocities and positions, and these updated fields are then used to advance the velocities and positions of the particles over the following time step.

In the present study, a single space coordinate z, in the direction of propagation, is considered. The particles are sheets perpendicular to the z direction. They have, however, velocities in all three directions, v_x , v_y , v_z , so that the distribution function must be defined over a four-dimensional phase space. The electromagnetic fields are solved from Maxwell's equations, not including the transverse component of the displacement current. The simulation takes account only of electrons, the ions contributing only a neutralizing background charge. In the computation to be shown the time step varied from $0.2 \omega_p^{-1}$ to $0.4 \omega_p^{-1}$ and the number of particles used in the simulation varied from 30 000 to 500 000 depending on the complexity of the system and the grid size used to define the initial distribution function. Because of the large number of wavelengths contained in wavepackets of interest in VLF emissions it is not feasable to simulate the entire inhomogeneous problem or to use the actual parameters relevant to the magnetosphere. However, it is possible to simulate different aspects of the problem with such parameters that enable the effects we seek to be observed within a reasonable length of computation.

The first study is devoted to showing the existence of an instability due to phase-correlated particles. A large amplitude whistler wave is set up in a thermal plasma at t = 0, by giving specified perturbations in transverse velocity to the individual electrons. This wave corresponds to mode n =5-in other words, to a wavelength equal to one fifth of the system's length. In addition to this wave an initial "noise" spectrum is also introduced with energies equally distributed among modes n = 1 through 20. To provide an ample supply of resonant particles, we assume the electron population to be 100% energetic. wave damps initially due to cyclotron damping (figure 5); then its amplitude oscillates with a period $\tau_{\rm T} = 30 \ \omega_{\rm p}^{-1}$, which corresponds approximately to the trapping frequency ω_T derived earlier. After several trapping periods the amplitude of this modulation decays,



The propagation of a whistler wave-packet, shown as a numerical simulation in an unstable medium and demonstrating the nonlinear spreading. The plasma has a 10% energetic electron population with unstable loss-cone distribution, with $\theta_{\rm loss\ cone}=60$ deg, $\langle v^2\rangle^{1/2}=c/3,\ \omega/\Omega=0.5$ and $\Omega/\omega_{\rm p}=0.5$. Starting from a small amplitude the wavepacket first propagates according to linear theory while being amplified by the loss-cone instability. At $\omega_{\rm p}t=80$ the wavepacket reaches an amplitude sufficient to trap resonant electrons travelling from left to right, and as these electrons emerge at the rear of the wavepacket they emit new waves as shown at $\omega_{\rm p}t=120$ and 160. Note that the amplitude continues to increase throughout the run, the energy being provided by resonant electrons with $v_{\rm p}>0$ that gradually fill the loss cone.

and the wave settles to an approximate steady state described by Richard Lutomirski and Sudan. However, this state is not stable, and new waves are amplified from the noise level. We observe that both the lower sideband (n=1 through 4) and the upper sideband (n=6 through 9) grow at approximately the same rate $(\gamma \simeq 0.01 \omega_{\rm p})$ and in a few hundred $\omega_{\rm p}^{-1}$ become comparable in amplitude to the main wave. The spectrum at $\omega_{\rm p} t = 260$ is approximately symmetric in agreement with the symmetry of the growth rates shown in figure 4.

Phase plots of the resonant electrons at different times are shown in figure 6. The phase correlation of the transverse velocity of resonant electrons is shown clearly on the plots of ϕ versus z at $\omega_p t = 10$ and 20. It disappears at $\omega_p t = 30$, which corresponds to a completed trapping oscillation, reappears at $\omega_p t = 40$ and for longer

times continues to oscillate with the main wave amplitude. The plots of v_{\parallel} versus z show the formation of trapping vortices due to the spreading of electrons along closed lines of constant energy in the potential well of the wave.

Our second study concerns the nonlinear spread of a wavepacket in the direction in which phase correlated electrons emerge. We examined first the propagation of a wavepacket in the absence of trapped particles, and in this case the propagation velocity and spread in the wavepacket checked quite well with calculations based on linear dispersion. We consider next the evolution of a small-amplitude wavepacket of similar shape through a plasma having a 10% energetic electron population with an unstable loss-cone velocity distribution, figure 7. From $\omega_{\rm p}t = 0$ to $\omega_{\rm p}t = 80$ the wavepacket propagates with only minor distortion, its amplitude increasing according to the growth rate predicted by linear theory. At $\omega_{\rm p}t$ = 80 the amplitude reaches a level such that the resonant electron transit time T approaches the mean trapping time $2\pi/\langle \omega_{\rm T} \rangle$ and the tail of the packet begins to extend. Notice that the front of the packet is unchanged, which indicates that this effect is not due to linear dispersion. The velocity distribution reinforces this point; not much change occurs in particles with $v_{\parallel} < 0$, but there is a considerable rearrangment of the distribution for $v_{\parallel} > 0$. These runs show conclusively that resonant phase-correlated particles do indeed emerge from the wavepacket without serious loss of phase-correlation to generate new

In summary the physical process by which VLF emissions occur may be stated roughly as follows. The triggering wavepacket is amplified by the resonant electrons of a nonthermal population of energetic electrons. When the wave amplitude increases it reacts on these electrons by aligning their phase to form a circularly polarized transverse current. These electrons, because they are moving counter to the wave group velocity, leave the original wavepacket but without significant loss of phase-correlation. New waves of

References

OF

1

10

and

lite!

cket I

10

1000

t de

18

side 1

amp

伽

distor

- R. A. Helliwell, Whistlers and Related Ionospheric Phenomena, Stanford U. P. (1965).
- L. R. O. Storey, Phil. Trans. Roy. Soc. (London). A 246, 113 (1953). The properties of the whistler mode are discussed in any standard text on wave propagation in ionized media; see for example J. A. Ratcliffe, The Magneto-Ionic Theory and its Application to the Ionosphere, Cambridge U. P., (1959).
- 3. R. L. Smith, J. Geophys. Res. 66, 3699 (1961).
- R. A. Helliwell, J. Geophys. Res. 68, 5387 (1966).
- R. A. Helliwell, J. Katsufrakis, M. Trimpi, N. Brice, J. Geophys. Res. 69, 2391 (1964).
- R. Gallet, R. A. Helliwell, J. Res. Nat. Bur. Stand., 63D (1), 21 (1959); R. L. Dowden, J. Geophys. Res. 67, 1745 (1962).
- 7. O. Buneman, Phys. Rev. 115, 503 (1959).
- N. Brice, "Discrete very-low-frequency emissions from the upper atmosphere," Report No. SEL 64-088, Stanford Electronics Lab. Stanford U. (1966); J. Geophys. Res. 68, 4626 (1960).
- R. A. Helliwell, J. Geophys. Res. 72, 4773 (1969).
- R. N. Sudan, E. Ott, Bull. Am. Phys. Soc. 14, 1039 (1969); J. Geophys. Res. 76, 4463 (1971).
- J. A. Van Allen, J. Geophys. Res. 64, 1683 (1959).
- R. Z. Sagdeev, V. D. Shafranov, Zh. Eksp. Teor. Fiz. 39, 181 (1961), Eng.

different frequencies are emitted through an instability driven by these phase-correlation electrons. These frequencies are determined from the resonance condition and the spatially varying magnetic field.

Much remains to be done in applying these ideas to other classes of VLF emissions, and in particular some of the details of frequency-time characteristics are not completely understood. However, the fundamental premise that these emissions occur because of wave-particle resonance is well established.

We are indebted to Neil Brice and Edward Ott for many discussions on the subject matter of this article.

Sudan's work was supported by the Atmospheric Sciences Section, National Science Foundation under grant GA-35530X; Denavit was supported jointly by the USAEC under contract AT(11-1)-2200 and the Office of Naval Research Contract N00014-67-A-0356-0026. Acknowledgment is made to the National Center for Atmospheric Research, which is sponsored by the National Science Foundation, for computer time in this research.

This article is based on an invited talk given by Sudan at the Symposium on Plasma Physics, New York meeting of the APS, 29 January 1973.

- trans.: Sov. Phys.—JETP 12, 130 (1961).
- 13. R. N. Sudan, Phys. Fluids 6, 57 (1963).
- 14. P. D. Noerdlinger, Ann. Phys. (NY) 22, 12 (1963).
- T. Bell, O. Buneman, Phys. Rev. 133, 25 (1964).
- T. Rosenberg, R. A. Helliwell, J. Katsufrakis, J. Geophys. Res. 76, 8445 (1971).
- C. F. Kennel, H. E. Petschek, J. Geophys. Res. 71, 1 (1966).
- J. Dungey, Planet. Space Sci. 11, 591 (1963).
- R. Lutomirski, R. N. Sudan, Phys. Rev. 147, 156 (1966).
- K. I. Gringauz, Rev. of Geophys. 7, 339 (1969);
 D. A. Gurnett, L. A. Frank, J. Geophys. Res. 78, 145 (1973).
- 21. K. B. Dysthe, J. Geophys. Res. 76, 6915
- D. Nunn, Planet. Space Sci. 19, 1141 (1971).
- N. I. Budko, V. I. Karpman, O. A. Pokhotelov, Cosmical Electrodynamics 3, 147 (1972).
- 24. T. Gold, Nature 218, 731 (1968).
- 25. See ref. 7; J. Dawson, Phys. Fluids 5, 445 (1962); J. Denavit, W. L. Kruer, Phys. Fluids 14, 1782 (1971). A number of review papers on computer simulation of plasmas may be found in Methods of Computational Physics, Vol. 9, Academic, New York (1970) and Proc. IVth Conf. on Numerical Simulation of Plasmas (J. Boris, R. Shanny, eds.) Naval Research Laboratory, Washington, D.C. (1970).



1 OMA = 500 Photomultipliers!

SSRI's OMA (Optical Multichannel Analyzer) takes a digital electronic photograph of your dispersed spectrum and displays it in real time. Quantitative access to 500 channels of spectral data is available immediately with OMA. Opens new horizons in such fields as: Multielement Analysis; Flash Lamp Analysis; Laser Diagnostics; Astronomical Spectrometry.



New OMA brochure outlines other applications, operating modes, specifications, accessories and prices. Write for your free copy today.

 Mail literat My applicatio 		
Name		
Firm		
Address		
City	State	Zíp
CE	INSTRUM	IENTS C